Effective Medium Theory for Kapitza Stratified Media: Diffractionless Propagation

Carlo Rizza[1,2] and Alessandro Ciattoni[2]

[1]*Dipartimento di Scienza e Alta Tecnologia, Università dell'Insubria, Via Valleggio 11, 22100 Como, Italy*
[2]*Consiglio Nazionale delle Ricerche, CNR-SPIN, 67100 Coppito L'Aquila, Italy*

(Received 28 September 2012; published 3 April 2013)

We show that in the presence of a rapidly modulated dielectric permittivity with a large modulation depth (Kapitza medium) a novel and robust regime of diffractionless electromagnetic propagation occurs. This happens when the mean value to depth ratio of the dielectric profile is comparable to the small ratio between the modulation period and the wavelength. We show that the standard effective medium theory is inadequate to describe the proposed regime and that its occurrence is not substantially hampered by medium losses. We check the feasibility of the proposed regime by means of a large modulation depth metal-dielectric layered medium whose electromagnetic behavior is analytically investigated.

DOI: 10.1103/PhysRevLett.110.143901 PACS numbers: 42.25.Bs, 41.20.Jb, 42.30.Wb, 78.20.Ci

Subwavelength imaging and diffractionless propagation are major photonics subjects that have attracted, in the past decade, a renewed research interest triggered by the advent of metamaterials [1,2] since a negative index metamaterial slab was shown to support an overall superlensing effect. Remarkably, without resorting to exotic and hardly available magnetic properties, it has been realized that a metal slab can provide subwavelength imaging as well [3,4]. A refinement of such a superlens has been proposed in the form of a metal-dielectric layered composite obtained by alternating two materials with permittivities whose real parts have opposite signs [5,6]. Different superlensing mechanisms occur in the canalization regime [7–10] and in hyperbolic metamaterials [11–15].

In this Letter we show that a novel regime of diffractionless propagation occurs for transverse magnetic (TM) waves propagating, in the long wavelength regime, through rapidly modulated stratified media with a large dielectric modulation depth (Kapitza media). The considered electromagnetic situation is conceptually equivalent to that of the mechanical inverted pendulum whose pivot point is subjected to high-frequency vertical oscillations (Kapitza pendulum) [16,17], since these oscillations produce a rapidly varying contribution to the Lagrangian function with a large modulation depth. The concept has been successfully extended and implemented in the general context of quantum and nonlinear physics [18–27]. In all the situations, even though the system is not able to follow the rapid external oscillations, these are still able to affect the average system dynamics by means of additional slowly varying potential contributions (e.g., the rapid external oscillations yield the stabilization of the inverted state of the mechanical pendulum). In the electromagnetic situation that we consider in this Letter, the rapid and deep dielectric spatial modulation entails the diffractionless propagation of the averaged electromagnetic field.

The electromagnetic field amplitudes $\mathbf{E} = E_x(x, z)\hat{\mathbf{e}}_x + E_z(x, z)\hat{\mathbf{e}}_z$, $\mathbf{H} = H_y(x, z)\hat{\mathbf{e}}_y$ associated with monochromatic TM waves satisfy Maxwell's equations

$$-\partial_x E_z + \partial_z E_x = i\omega\mu_0 H_y, \qquad \partial_z H_y = i\omega\epsilon_0\epsilon_x E_x, \qquad \partial_x H_y = -i\omega\epsilon_0\epsilon_z E_z, \tag{1}$$

where $\boldsymbol{\epsilon} = \mathrm{diag}[\epsilon_x, \epsilon_y, \epsilon_z]$ is the medium relative dielectric tensor and the time dependence $e^{-i\omega t}$ has been assumed. Here we consider a specific medium periodically modulated along the z axis whose dielectric permittivity $\epsilon_x = \epsilon_z = \epsilon$ admits the Fourier series expansion

$$\epsilon = \epsilon_m + \sum_{n\neq 0}\left(a_n + \frac{b_n}{\eta}\right)e^{in(K/\eta)z}, \tag{2}$$

where ϵ_m and $(a_n + b_n/\eta)$ are the Fourier coefficients whereas $2\pi\eta/K$ is the spatial period. Here η is a dimensionless parameter that we have introduced to explore the asymptotic electromagnetic behavior pertaining to the limit $\eta \to 0$ where both the grating amplitude and its spatial frequency are very large (assuming that $K \approx k_0 = \omega/c$). Note that the coefficients a_n account for a contribution to the modulation which is not large, and it is essential for allowing the model to avoid unrealistic features as a permittivity imaginary part rapidly oscillating between large negative and positive values. Since electromagnetic propagation is here characterized by two very different scales (i.e., the radiation wavelength and the permittivity modulation period), it is natural to let each electromagnetic field component separately depend on z and $Z = z/\eta$ (multiscale technique where Z is the fast coordinate [28]) and to represent it as a Taylor expansion up to first order in η, i.e.,

$$A(x, z, Z) = [\bar{A}^{(0)}(x, z) + \tilde{A}^{(0)}(x, z, Z)] + \eta[\bar{A}^{(1)}(x, z) + \tilde{A}^{(1)}(x, z, Z)], \tag{3}$$

where $A = E_x$, E_z, or H_y, the superscripts (0) and (1) label the order of each term whereas the overline and the tilde label the averaged and rapidly varying contributions to each order, respectively. Substituting the field components of this form into Eqs. (1), each equation yields a power series in η whose various orders are evidently the

superposition of a slowly varying (independent of Z) and a fast (dependent on Z) contribution, all of which can be independently balanced. From the lowest order (which is here η^{-1}) we obtain $\tilde{E}_x^{(0)} = 0$, $\bar{E}_z^{(0)} = 0$, $\tilde{E}_z^{(0)} = 0$, and $\tilde{H}_y^{(0)} = (\omega\epsilon_0/K)\sum_{n\neq 0}(b_n/n)e^{inKZ}\bar{E}_x^{(0)}$, or, in other words, the dominant contribution to the x component of the electric field is slowly varying, whereas the z component of the electric field has no zeroth order. The order η^0 of the first of Eqs. (1) yields

$$\partial_z \bar{E}_x^{(0)} = i\omega\mu_0 \bar{H}_y^{(0)} \tag{4}$$

and $\partial_Z \tilde{E}_x^{(1)} = i\omega\mu_0 \tilde{H}_y^{(0)}$, which in turn, with the help of the obtained expression for $\tilde{H}_y^{(0)}$, yields $\tilde{E}_x^{(1)} = (k_0^2/K^2)\sum_{n\neq 0}(b_n/n^2)e^{inKZ}\bar{E}$. The slowly varying part of the order η^0 of the second of Eqs. (1), together with the obtained expression for $\tilde{E}_x^{(1)}$ yield

$$\partial_z \bar{H}_y^{(0)} = -i\omega\epsilon_0\epsilon_{\text{eff}}\bar{E}_x^{(0)}, \tag{5}$$

where

$$\epsilon_{\text{eff}} = \epsilon_m + \frac{k_0^2}{K^2}\sum_{n\neq 0}\frac{b_{-n}b_n}{n^2}. \tag{6}$$

To summarize we have obtained that the leading term of the TM electromagnetic field is slowly varying and transverse electromagnetic (TEM), i.e., $\mathbf{E} \simeq \bar{E}_x^{(0)}(x,z)\hat{\mathbf{e}}_x$, $\mathbf{H} \simeq \bar{H}_y^{(0)}(x,z)\hat{\mathbf{e}}_y$, and, in addition, its components satisfy Eqs. (4) and (5) so that the field undergoes diffractionless propagation and experiences the uniform effective permittivity ϵ_{eff}.

As for any effective medium theory (EMT), the field is here slowly varying since it cannot follow the rapid medium dielectric modulation. However, the fact that the longitudinal component vanishes is a very unique and important feature of the proposed regime which has a simple physical explanation arising from the combination of the first Maxwell equation and the large depth of the dielectric modulation. In fact, a very deep and rapidly modulated dielectric response would produce volume polarization charges too strong to be screened by the electric field, an incompatibility avoided by the condition $E_z \simeq 0$. For example, assuming $\epsilon = \epsilon_m + (b/\eta)\cos(Kz/\eta)$, the equation $\nabla\cdot\mathbf{D} = 0$ yields $\epsilon(\partial_x E_x + \partial_z E_z) - (bK/\eta^2)\times \sin(Kz/\eta)E_z = 0$ from which it is evident that, since the first term self-consistently scales as $1/\eta$, E_z has to be proportional to η for mitigating the divergence of the factor $1/\eta^2$ in the second term. The diffractionless propagation of the leading contribution to the electromagnetic field in the considered regime is a consequence of its TEM structure since, as is well known, TM waves with vanishing longitudinal components do not undergo diffraction [as is evident from Eqs. (1)]. It should be stressed that the superresolution mechanisms reported in the literature are based on the requirement that $\epsilon_z \to \infty$ [since, when combined with the third of Eqs. (1), this condition yields $E_z \to 0$ and hence diffractionless propagation], a condition that has to be fulfilled by exploiting the standard EMT and which is essentially hampered by medium absorption [8]. On the other hand, in the regime we are investigating here, the longitudinal effective permittivity ϵ_z is not even defined and it is evident from the above presented multiscale analysis that the longitudinal field component E_z vanishes regardless of the medium losses (since we have not assumed the permittivity to be real). We conclude that the occurrence of diffractionless propagation within Kapitza stratified media is very robust and substantially not hampered by medium losses. Note that, in analogy to the potential governing the averaged dynamics of the Kapitza pendulum, the effective permittivity of Eq. (6) is the sum of the average permittivity plus a contribution arising from the rapidly varying part of the dielectric modulation. Such an effective medium response, together with the TEM field structure, clarifies that the effective medium theory we are considering here (Kapitza EMT) is fundamentally different from the standard effective medium theory (standard EMT) for layered media whose main result is that the effective principal permittivities are $\epsilon_x = \langle\epsilon\rangle = \epsilon_m$ and $\epsilon_z = \langle\epsilon^{-1}\rangle^{-1}$. The difference between the two regimes is also assured by the fact that the standard effective medium results can be simply derived by using the above discussed multiscale technique in the presence of the dielectric profile of Eq. (2) with $b_n = 0$, i.e., without the large modulation depth contribution to the permittivity. Remarkably, the improvement of the standard EMT contained in the approach of Elser *et al.* in Ref. [29], also clearly shows that the standard EMT is not adequate when the modulation depth is large, a condition characterizing the Kapitza EMT discussed in the present Letter [30].

In order to check the predictions of the proposed Kapitza EMT, we have considered the reflection and transmission of TM plane waves from a slab filled by a Kapitza stratified medium, as sketched in Fig. 1(a). The dielectric modulation is along the z axis with period $\eta\lambda$ where $\lambda = 2\pi/k_0$ is the vacuum radiation wavelength and η is the above introduced small parameter, whereas the slab thickness L is a multiple of the period $\eta\lambda$. The unit cell comprises N homogeneous layers of thicknesses $\eta\lambda/N$ and the dielectric permittivity of the jth layer ($j = 1, ..., N$) is

$$\epsilon_j = \epsilon_m + \left(\frac{1}{\eta} + i\delta\epsilon\right)\cos\left[\frac{2\pi}{N}(j-1)\right], \tag{7}$$

where ϵ_m is the mean value of the dielectric permittivity and $\delta\epsilon$ is responsible for the (not large) modulation of medium absorption. The corresponding profile of the slab dielectric permittivity is evidently of the kind of Eq. (2) (with $K = k_0$) and its real and imaginary parts are sketched, within a unit cell, in Figs. 1(b) and 1(c), respectively [where $\epsilon_m' = \text{Re}(\epsilon_m)$ and $\epsilon_m'' = \text{Im}(\epsilon_m)$]. The check of the Kapitza EMT has been performed by choosing

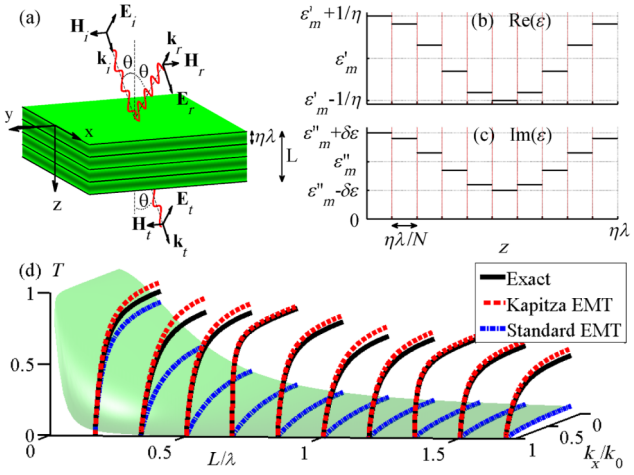

FIG. 1 (color online). (a) Layered slab and TM waves scattering geometry. (b), (c) Real and imaginary parts of the dielectric permittivity profile within the unit cell. (d) Comparison between the exact slab transmissivity (solid lines) and those predicted by the Kapitza (dashed lines) and the standard EMT (dash-dotted lines and semitransparent interpolating surface).

$\lambda = 100\ \mu$m, $\epsilon_m = 0.05 + 0.05i$, $\delta\epsilon = 0.025$, $N = 10$, and $\eta = 1/60$, which is a realistic situation since $-60 < \mathrm{Re}(\epsilon) < 60$ and $0.025 < \mathrm{Im}(\epsilon) < 0.075$ (thus avoiding the use of active media) and since the layers' thickness $\eta\lambda/N \simeq 166$ nm is fully feasible. The scattering process of TM waves by the considered layered medium admits a full analytical description (by means of the transfer-matrix method) and in Fig. 1(d) we have plotted the exact profiles (solid line) of the transmissivity defined as $T = |\mathbf{E}_t|^2/|\mathbf{E}_i|^2$ [see Fig. 1(a) for the definition of the field amplitudes] as a function of the transverse wave vector $k_x = k_0 \sin\theta$ for various slab thicknesses L. On the other hand, Eqs. (4) and (5) are easily solved to yield the transmissivity

$$T = |\cos(k_z L) - iF \sin(k_z L)|^{-2}, \tag{8}$$

where $k_z = k_0\sqrt{\varepsilon_{\mathrm{eff}}}$ and $F = [\sqrt{\varepsilon_{\mathrm{eff}}}\cos\theta + 1/(\sqrt{\varepsilon_{\mathrm{eff}}}\cos\theta)]/2$. After evaluating the Fourier coefficients of the considered dielectric profile, Eq. (6) yields $\epsilon_{\mathrm{eff}} = 0.5339 + 0.05i$ and in Fig. 1(d) we have reported various profiles (dashed lines) of the resulting transmissivity of Eq. (8) pertaining to the Kapitza EMT. In addition, the standard EMT would describe the slab as an anisotropic medium with dielectric permittivities $\epsilon_x = \langle\epsilon\rangle = 0.05 + 0.05i$ and $\epsilon_z = \langle\epsilon^{-1}\rangle^{-1} = (-7.205 + 7.194i) \times 10^3$ and, in Fig. 1(d), we have plotted various profiles (dash-dotted lines) of the the corresponding transmissivity which coincides with Eq. (8) with $k_z = k_0\sqrt{\epsilon_x(1 - \frac{\sin^2\theta}{\epsilon_z})}$ and $F = \frac{1}{2}(\frac{k_0\epsilon_x\cos\theta}{k_z} + \frac{k_z}{k_0\epsilon_x\cos\theta})$. Note that the agreement between the exact predictions and those based on the Kapitza EMT is remarkable whereas the standard EMT completely fails. It is interesting to note that in the considered situation the ratio between the layer thicknesses $\eta\lambda/N$ and the smallest layer wavelength, approximately $\sqrt{\eta}\lambda$, is $\simeq \sqrt{\eta}/N \simeq 0.013$ which is much smaller than one, a condition which assures the validity of the standard EMT in layered media when the modulation depth is not large.

It is well known that medium absorption plays a very detrimental role in the observation of the canalization regime [8] as well as on all the other mechanisms supporting diffractionless propagation. In order to investigate the effect of medium losses on the Kapitza regime we are discussing here, we have extended the scattering experiment of Fig. 1(a) to encompass even evanescent waves and we have evaluated, for a number of slabs characterized by different absorption efficiencies, the quantity $T = |\mathbf{E}_t|^2_{z=L}/|\mathbf{E}_i|^2_{z=0}$ as a function of the transverse wave vector k_x (which, for $|k_x| < k_0$, coincides with the above discussed slab transmissivity and, for $|k_x| > k_0$, entails information on the slab efficiency to transport evanescent waves). In Fig. 2 we report the exact logarithmic plot of T together with the corresponding profiles predicted by the Kapitza and the standard EMTs for three different slabs of thickness $L = 1.66\lambda$ which are identical to those considered in Fig. 1 but characterized by different values of ϵ_m and $\delta\epsilon$: (a) $\epsilon_m = 0.05 + 0.005i$, $\delta\epsilon = 0.0025$; (b) $\epsilon_m = 0.05 + 0.05i$, $\delta\epsilon = 0.025$; (c) $\epsilon_m = 0.05 + 0.5i$, $\delta\epsilon = 0.025$. The corresponding dielectric permittivities predicted by the Kapitza and the standard EMTs are (a) $\epsilon_{\mathrm{eff}} = 0.5339 + 0.0050i$, $\epsilon_x = 0.05 + 0.005i$, $\epsilon_z = (-14.256 + 1.424i) \times 10^3$; (b) $\epsilon_{\mathrm{eff}} = 0.5339 + 0.05i$, $\epsilon_x = 0.05 + 0.05i$, $\epsilon_z = (-7.205 + 7.194i) \times 10^3$; (c) $\epsilon_{\mathrm{eff}} = 0.5339 + 0.05i$, $\epsilon_x = 0.05 + 0.5i$, $\epsilon_z = (-0.154 + 1.425i) \times 10^3$. From Fig. 2 we note that in all the three considered situations the Kapitza EMT predictions largely agree with

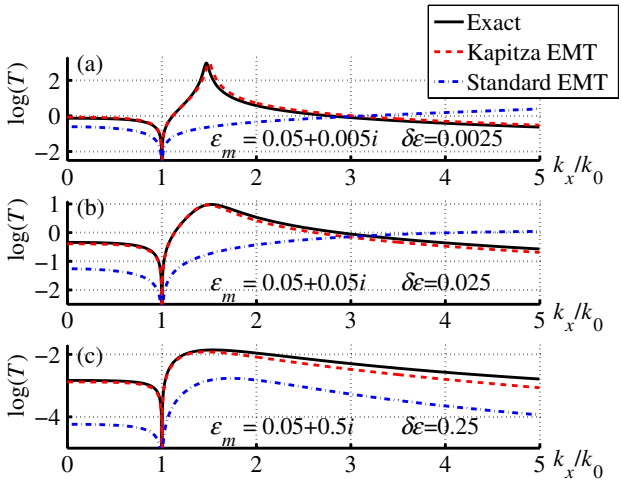

FIG. 2 (color online). Logarithmic plot of the quantity $T = |\mathbf{E}_t|^2_{z=L}/|\mathbf{E}_i|^2_{z=0}$, as a function of the transverse impinging momentum k_x, generalizing the slab transmissivity of Fig. 1(d) to encompass transport of evanescent waves for three slabs of thickness $L = 1.66\lambda$ and $\eta = 1/60$, with different mean values and modulation depths of the permittivity imaginary part.

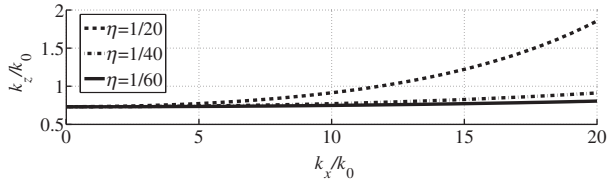

FIG. 3. Equifrequency contour of the considered Kapitza stratified medium for different values of η.

the exact phenomenology whereas the standard EMT is inadequate and, most importantly, that this happens almost regardless of the medium absorption. Considering that in panel (c) of Fig. 2 the mean value and the modulation depth of the permittivity imaginary part are 100 times greater than those of panel (a) of Fig. 2, we restate that the Kapitza regime is very robust against medium losses, a very distinct and important feature which does not characterize the other diffractionless propagation regime presented in the literature.

From Fig. 2, it should also be stressed that the agreement between the Kapitza EMT and the exact phenomenology is, in the considered situation, very good and robust even for evanescent waves ($|k_x| > k_0$), an essential requirement for achieving super resolution. As a further validation of this statement, in Fig. 3 we plot the exact equifrequency contour (EFC) of some typical Kapitza media [see Eq. (7)] with $\epsilon_m = 0.05$ and $\delta\epsilon = 0$ at $\lambda = 100$ μm obtained by imposing the Bloch condition on the field amplitudes evaluated through the transfer-matrix method [29]. Note that both the $\eta = 1/40$ and the $\eta = 1/60$ EFCs are very flat over a large portion of the evanescent wave spectrum. On the other hand the $\eta = 1/20$ EFC effectively deviates from the constant nondiffracting value of k_z roughly for $|k_x| > 5k_0$ and therefore diffraction is expected to be not fully suppressed. Even though we have mainly focused on the novel diffractionless propagation regime, it is worth checking the subwavelength imaging features of a Kapitza layered slab. Specifically we have considered a slab whose unit cell has the dielectric distribution of Eq. (7) with $\epsilon_m = 0.05 + 0.005i$, $\delta\epsilon = 0.0025$, $N = 10$, and $\eta = 1/60$ [thus coinciding with the case of Fig. 2(a)]. The radiation wavelength is $\lambda = 100$ μm and the unit cell thickness is $\Lambda = \eta\lambda = 1.67$ μm. We have considered a slab with $M = 82$ unit cells since its resulting width $L = M\Lambda = 135.66$ μm is very close to the width $L_F = \lambda/\sqrt{\mathrm{Re}(\epsilon_{\mathrm{eff}})} = 136.85$ μm for which the Kapitza homogeneous slab governed by Eqs. (4) and (5) with $\epsilon_{\mathrm{eff}} = 0.5339 + 0.005i$ [from Eq. (6)] has its second Fabry-Perot resonance. Using the transfer-matrix method, we have evaluated the slab point-spread-function PSF(x) according to which the transmitted magnetic field profile $H_y^{(T)}(x, L)$ can be expressed as the convolution of PSF(x) with the incident magnetic field $H_y^{(I)}(x, 0)$, or $H_y^{(T)}(x, L) = \mathrm{PSF}(x) * H_y^{(I)}(x, 0)$ [31]. In Fig. 4(a) we plot the comparison

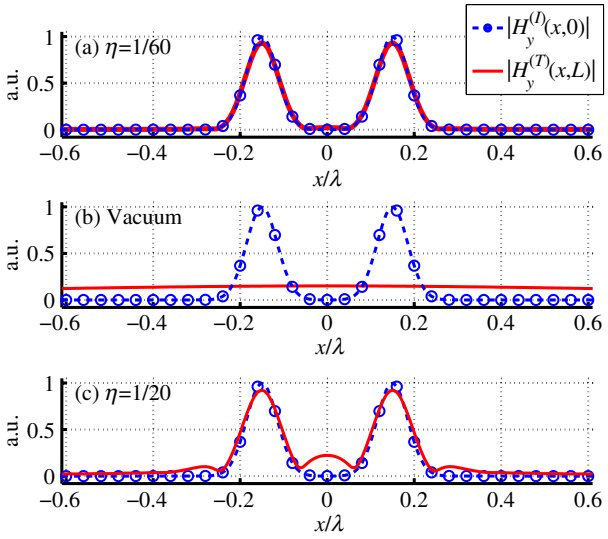

FIG. 4 (color online). (a) Imaging of a subwavelength two-peaked shape at $\lambda = 100$ μm by a Kapitza slab [as reported in Fig. 1(a) with the unit cell dielectric profile of Figs. 1(b) and 1(c)] characterized by $\epsilon_m = 0.05 + 0.005i$, $\delta\epsilon = 0.0025$, $N = 10$, $\eta = 1/60$, and $L = 135.66$ μm. (b) Diffraction of the subwavelength two-peaked shape after $L = 135.66$ μm vacuum propagation. (c) Same as in panel (a) but with $\eta = 1/20$.

between the slab output and input images for an impinging magnetic field whose profile consists of two Gaussians of equal width $\sigma = \lambda/20$ whose separation distance is 4σ, i.e., $H_y^{(I)}(x, 0) = H_0[e^{-(x-2\sigma)^2/\sigma^2} + e^{-(x+2\sigma)^2/\sigma^2}]$. Apart from a slight decrease of the peak's height due to medium absorption, the outcoming image is clearly a very accurate copy of the incoming one. To appreciate such an imaging result, we have reported in Fig. 4(b) the effect of vacuum propagation on the above incoming field, and the complete deterioration of the considered subwavelength image is evident. For completeness, in Fig. 4(c) we have plotted the analogous fields comparison for a slab identical to that of panel (c) of Fig. 2 but with $\eta = 1/20$ whose subwavelength imaging efficiency is evident even in the presence of a slight image deterioration resulting from the small sidelobes [32].

In conclusion, we have proposed and discussed a novel diffractionless propagation regime which is not fundamentally affected by medium losses and it is very robust against the tailoring of the medium dielectric properties. Diffraction suppression is here achieved through propagation in a medium whose dielectric permittivity is rapidly modulated with a large modulation depth so that the physical underpinnings of the proposed setup are in many respects an elaboration of those that in mechanics are associated with the stabilization of the inverted pendulum (the Kapitza pendulum, from which we take the name Kapitza EMT for our approach).

This research has been funded by the Italian Ministry of Research (MIUR) through the "Futuro in Ricerca" FIRB-Q98 Grant No. PHOCOS-RBFR08E7VA.

[1] V. G. Veselago, Sov. Phys. Usp. **10**, 509 (1968).
[2] J. B. Pendry, Phys. Rev. Lett. **85**, 3966 (2000).
[3] N. Fang, H. g Lee, C. Sun, and X. Zhang, Science **308**, 534 (2005).
[4] T. Taubner, D. Korobkin, Y. Urzhumov, G. Shvets, and R. Hillenbrand, Science **313**, 1595 (2006).
[5] J. B. Pendry and S. A. Ramakrishna, Physica (Amsterdam) **338B**, 329 (2003).
[6] S. A. Ramakrishna, J. B. Pendry, M. C. K. Wiltshire, and W. J. Stewart, J. Mod. Opt. **50**, 1419 (2003).
[7] P. A. Belov and Y. Hao, Phys. Rev. B **73**, 113110 (2006).
[8] X. Li, S. He, and Y. Jin, Phys. Rev. B **75**, 045103 (2007).
[9] X. Li and F. Zhuang, J. Opt. Soc. Am. A **26**, 2521 (2009).
[10] P. Li and T. Taubner, Opt. Express **20**, A11787 (2012).
[11] Z. Jacob, L. V. Alekseyev, and E. Narimanov, Opt. Express **14**, 8247 (2006).
[12] Z. Liu, H. Lee, Y. Xiong, C. Sun, and X. Zhang, Science **315**, 1686 (2007).
[13] H. Lee, Z. Liu, Y. Xiong, C. Sun, and X. Zhang, Opt. Express **15**, 15 886 (2007).
[14] B. D. F. Casse, W. T. Lu, Y. J. Huang, E. Gultepe, L. Menon, and S. Sridhar, Appl. Phys. Lett. **96**, 023114 (2010).
[15] S. Zhang, Y. Xiong, G. Bartal, X. Yin, and X. Zhang, Phys. Rev. Lett. **106**, 243901 (2011).
[16] P. Kapitza, J. Exp. Theor. Phys. **21**, 588 (1951).
[17] L. D. Landau and E. Lifshitz, *Course in Theoretical Physics. Mechanics* (Pergamon Press, Oxford, 1976), 3rd ed., Vol. 1.
[18] S. Rahav, I. Gilary, and S. Fishman, Phys. Rev. Lett. **91**, 110404 (2003).
[19] Y. S. Kivshar and K. H. Spatschek, Chaos Solitons Fractals **5**, 2551 (1995).
[20] N. Gronbech-Jensen, Y. S. Kivshar, and M. Salerno, Phys. Rev. Lett. **70**, 3181 (1993).
[21] A. Hasegawa and Y. Kodama, Opt. Lett. **15**, 1443 (1990).
[22] A. Hasegawa and Y. Kodama, Phys. Rev. Lett. **66**, 161 (1991).
[23] L. Torner, Opt. Lett. **23**, 1256 (1998).
[24] J. Atai and B. A. Malomed,Phys. Lett. A **298**, 140 (2002).
[25] F. K. Abdullayev, J. G. Caputo, R. A. Kraenkel, and B. A. Malomed, Phys. Rev. A **67**, 013605 (2003).
[26] H. Sakaguchi and B. A. Malomed, Phys. Rev. E **70**, 066613 (2004).
[27] M. Centurion, M. A. Porter, P. G. Kevrekidis, and D. Psaltis, Phys. Rev. Lett. **97**, 033903 (2006).
[28] J. A. Sanders and F. Verhulst, *Averaging Methods in Nonlinear Dynamical Systems* (Springer-Verlag, Berlin, 1985).
[29] J. Elser and V. A. Podolskiy, Appl. Phys. Lett. **90**, 191109 (2007).
[30] Note that in the approach of Ref. [29] the modulation depth is not explicitly considered large. In addition, the advantages of our Kapitza approach compared to those of Ref. [29] are that the general analysis is here performed on the full Maxwell system without resorting to the layered medium model (as done in Ref. [29]) and that our reasoning can be easily extended to encompass possible medium nonlinearities.
[31] R. Kotyński and T. Stefamiuk, J. Opt. A: Pure Appl. Opt. **11**, 015001 (2009).
[32] Note that at the wavelength $\lambda = 100\ \mu$m, the values of the layers' dielectric permittivities considered in the example are realistic. On the other hand, even though at optical frequency layers with very large positive dielectric permittivity are not available, the maximum allowed optical permittivity (about 10) yields an intermediate regime where the proposed Kapitza mechanism, even though not fully operative, nevertheless yields quasidiffractionless propagation.